2016
International Symposium on Power Electronics,
Electrical Drives, Automation and Motion

Implementation of VVVF Drive for a Three Phase Induction Machine

Joon Sung Park[1], Byong Jo Hyon[1], Jin-Hong Kim[1], Jun-Hyuk Choi[1]
[1]Intelligent Mechatronics Research Center
Korea Electronics Technology Institute
203-101 Bucheon-TP B/D 388, Songnae-daero, Wonmi-gu
Bucheon-si, Gyeonggi-do, Korea, 420-733
Email : parkjs@keti.re.kr

***Abstract*—This paper presents the design and implementation of induction machine drives by estimating a slip in fluid load and the Variable Voltage Variable Frequency (VVVF) drive scheme based on Sinusoidal Pulse Width Modulation (SPWM) technique for a three phase induction motor has been applied for use. The work involves implementation of a closed-loop control scheme for an induction motor. The VVVF technique is used extensively in the industry as it provides the accuracy required at minimal cost. For the slip estimation, a value of the stator flux is accordingly required. However estimating stator flux is complicated and even adopting flux sensors increase the cost. In this paper, complex and economic problems are solved by simplified slip estimation and VVVF control. The analysis is made with 3.2kW induction motor which used for fluid load. The implementation of VVVF drive applied simplified slip estimation is proposed and its validity is demonstrated by experimental results**

Keywords—VVVF; SPWM; Inverter; Slip estimation; Induction machine(IM)

I. INTRODUCTION

The induction machine(IM)s are widely used in the electrical drives. The efficiency of motors in fluid load is lower than others since the IMs for fluid load have large air-gap to make vacuum state [1, 2]. It is necessary to make vacuous in the semiconductor fabrication [3]. The capacity of pump to keep vacuum state is usually small. Though it needs big capacity, it is settled to use multi-stage scheme. To make motor drive for vacuum pump, there are lots of schemes. In this application, key features are performance and cost. The first point to be discussed is to increase the performance of an inverter. For the performance, voltage must be utilized as much as it could. In this paper, sinusoidal pulse width modulation (SPWM) and VVVF scheme are applied because of easy and low cost way to implement. However the output voltage of SPWM is less than SVPWM as 15.5%. To increase voltage utilization, over-modulation is applied. To distinguish over-load condition, we need additional control method in VVVF control. The technique of Beck [4] relies on the steady-state equivalent circuit model. It obtains the rotor slip from a theoretical relationship between the slip and the phase delay angle of stator current relative to voltage. The method works for low slip operation only. However the IMs in fluid load need high slip operation because of large air-gap. In the method of Schauder [5] changes to the pseudo-flux definitions and speed adaption in order to extend the domain of asymptotic stability to lower speeds. It is complex to use and implement. In the case of sensor-less vector control drives, current information by current sensor is important, since the flux and the slip are estimated by the current information. Therefore hall sensor is usual for current sensor, but hall sensor lead to complexity and has cost problem. It is irrelevant to the main object. The microprocessor of space vector control receives and calculates all information, which are phase current, dc-link voltage, etc, in every PWM frequency. It, therefore, needs powerful microprocessor. Even though today's microprocessors are becoming more and more powerful, the cost of microprocessors for space vector control is still much higher. Microprocessor and current sensor for motor drives are critical role according to the cost. In this application, it is not that the vacuum pump works at variable speed, but it always works at the rated speed. Hence, VVVF control drives are good enough under this condition. But it needs more torque to make vacuous when indraft of air is occurred. In the case of VVVF control drives, because it is basically open-loop system, we need a method to distinguish what has been explained above.

In the literature, various methods have been proposed for slip estimation [5]-[9]. The techniques differ from each other by complexity, accuracy, etc. However, the majority of them are complex and use sensor-less vector control scheme. In this paper, based on simplified equivalent circuit of an induction machine, we derive the slip estimation to make vacuous.

II. PWM VOLTAGE SOURCE INVERTER

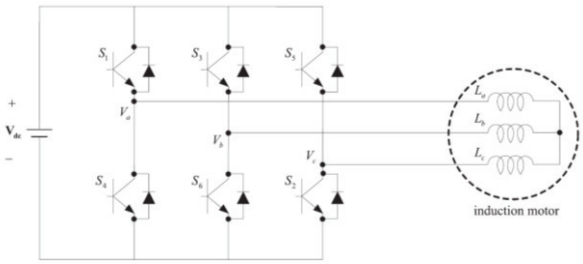

Fig. 1. Voltage source inverter.

978-1-5090-2067-6/16/$31.00 ©2016 IEEE

Several voltage controlled PWM methods have been proposed in literatures [10]-[12] such as SPWM and SVPWM. The objective of all these methods is to generate a sinusoidal inverter output voltage. However SPWM provides an easy way to control voltage and frequency. The performance of SPWM with third harmonic injection is also comparable.

A. Sinusoidal PWM

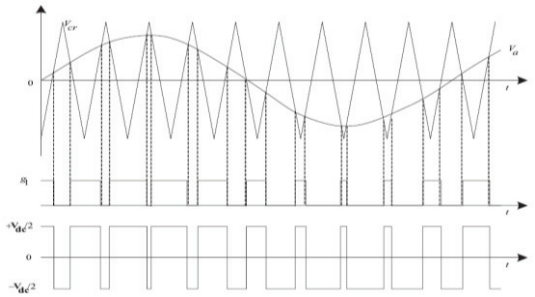

Fig. 2. Sinusoidal PWM.

SPWM aims at synthesizing motor voltages to produce currents as near to a sinusoid as economically possible. It operates from a fixed voltage dc source and combines both voltage control and frequency control within the inverter itself. There are three sinusoidal reference waves (V_a, V_b, V_c) each shifted by 120º. A carrier wave is compared with the reference signal corresponding to a phase to generate the gating signals for that phase. Comparing the carrier signal with the reference phase V_a, V_b, and V_c produces g_1, g_3, and g_5, respectively, as shown in Fig. 2. The amplitude modulation ratio M_a is defined as

$$M_a = \frac{V_{out}}{V_{cr}} \tag{1}$$

where V_{out} is the peak amplitude of the control signal. The amplitude V_{cr} of the carrier signal is generally kept constant. With SPWM, the maximum peak amplitude is linearly controlled in the range of $M_a \leq 1$.

B. Over-modulation

To increase the output voltage, the modulation ratio Ma must be increased beyond 1.0. The operation beyond d = 1.0 is called over-modulation. Over-modulation causes the output voltage to contain more harmonics in the sidebands as compared with the linear range (with $M_a \leq 1$). The amplitude of the fundamental frequency component dose not vary linearly with the amplitude modulation ratio M_a. The over-modulation region is avoided in uninterruptible power supplies because of a stringent requirement on minimizing the distortion in the output voltage. In induction motor drives, over-modulation is normally used [10]. For sufficiently values of M_a, the inverter voltage waveform degenerates from a PWM waveform into a square wave. From Fourier analysis, the peak values of the fundamental frequency and harmonic components in the inverter output waveform is obtained for a given input V_{dc} as

$$V_{out} = \frac{4}{\pi}\frac{V_{dc}}{2}. \tag{2}$$

However, square wave operation is feasible only in single-phase, full-bridge inverter circuit because of voltage cancellation [10].

C. 60-Degree PWM

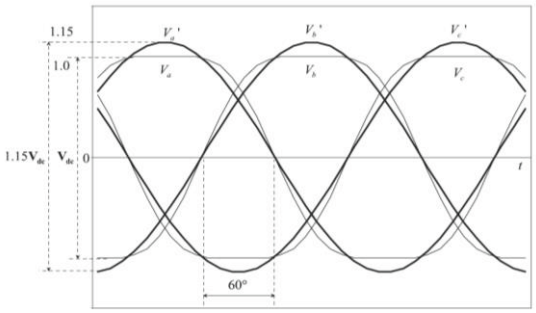

Fig. 3. Output waveforms for 60-degree PWM.

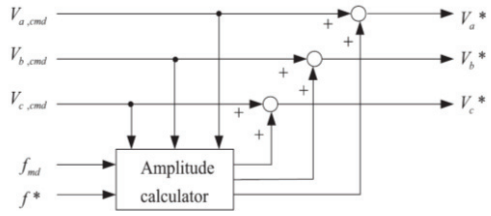

Fig. 4. Control scheme for over-modulation.

The 60º PWM is similar to the modified PWM. The idea behind 60º PWM is to flat top the waveform from 60º to 120º and 240º to 300º. The power devices are held on for one-third of the cycle at full voltage and have reduced switching losses. All triple harmonics such as 3rd, 9th, 15th, 21st, etc are absent in the three-phase voltages. The output is expressed as

$$V_{out} = \frac{2}{\sqrt{3}}\sin x + \frac{1}{2\pi}\sin 3x + \frac{1}{60\pi}\sin 9x + \cdots. \tag{3}$$

The output waveform is shown in Fig. 3. From equation (3), a fundamental magnitude of 60º PWM is $2/\sqrt{3}$ and this is approximately 1.15 times larger than SPWM. Thus the 60-degree PWM creates a larger fundamental and utilizes more of the available da voltage than does SPWM [12]. The control scheme for over-modulation is shown in Fig. 4 where f_{md} is the frequency when the peak amplitude is made as SPWM and $V_{a,cmd}$, $V_{b,cmd}$, and $V_{c,cmd}$ are target amplitudes of phase voltages, respectively. The amplitude calculator creates amplitudes in comparison with the frequency.

III. Mathematical Modelling of Induction Motors

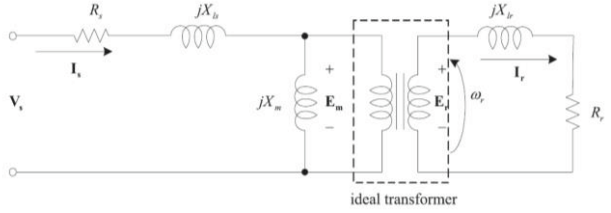

Fig. 5. Per-phase equivalent circuit of 3-phase induction motors.

For many practical purpose, a sufficiently accurate equivalent circuit is obtained by means of an approximation already employed in the case of single-phase transformers and also the terms of stator winding resistance R_s and stator leakage impedance $\omega_e L_{ls}$ are much smaller than magnetizing reactance $\omega_e L_{ls}$. Therefore the term of $\omega_e L_m$, is simply moved to the stator terminals. The approximate equivalent circuit can be shown in Fig. 6.

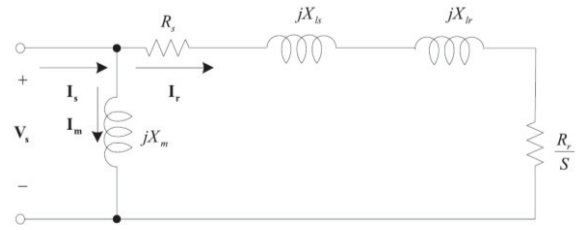

Fig. 6. Approximate equivalent circuit for analysis.

The total admittance at the angular frequency ω_e is

$$\mathbf{Y_s} = -j\frac{1}{\omega_e L_m} + \frac{1}{(R_s + R_r/S) + j\omega_e(L_{ls} + L_{lr})}$$
$$= \frac{(R_s + R_r/S)}{(R_s + R_r/S)^2 + \omega_e^2(L_{ls} + L_{lr})^2} - j[\frac{1}{\omega_e L_m} + \frac{\omega_e(L_{ls} + L_{lr})}{(R_s + R_r/S)^2 + \omega_e^2(L_{ls} + L_{lr})^2}]. \quad (4)$$

Thus, the input current $\mathbf{I_s}$ and the displacement angle are expressed as

$$\mathbf{I_s} = \mathbf{V_s}\mathbf{Y_s}$$
$$= \mathrm{Re}[\mathbf{I_s}] + j\,\mathrm{Im}[\mathbf{I_s}]$$
$$= \frac{(R_s + R_r/S)V_s}{(R_s + R_r/S)^2 + \omega_e^2(L_{ls} + L_{lr})^2} - j[\frac{V_s}{\omega_e L_m} + \frac{\omega_e(L_{ls} + L_{lr})V_s}{(R_s + R_r/S)^2 + \omega_e^2(L_{ls} + L_{lr})^2}], \quad (5)$$

$$\phi = \tan^{-1}(\frac{\mathrm{Im}[\mathbf{I_s}]}{\mathrm{Re}[\mathbf{I_s}]}), \quad (6)$$

And the output current $\mathbf{I_r}$ is

$$\mathbf{I_r} = \frac{(R_s + R_r/S)V_s}{(R_s + R_r/S)^2 + \omega_e^2(L_{ls} + L_{lr})^2} - j[\frac{V_s}{\omega_e L_m} + \frac{\omega_e(L_{ls} + L_{lr})V_s}{(R_s + R_r/S)^2 + \omega_e^2(L_{ls} + L_{lr})^2}]. \quad (7)$$

Substitution from (17), (10) in (13) then yields

$$T_e = 3\frac{p}{2}\frac{R_r}{S\omega_e}\frac{V_s^2}{(R_s + R_r/S)^2 + \omega_e^2(L_{ls} + L_{lr})^2}. \quad (8)$$

A typical relationship between speed and torque is determined from equation (8). At speed approaching synchronous speed, the slip S approaches zero, so that $R_r/S >> R_s$, and $R_r/S >> \omega(L_{ls}+L_{lr})$. Thus, from (8) below equations can be derived,

$$T_e \cong 3\frac{p}{2}\frac{S}{R_r}\frac{V_s^2}{\omega_e} \quad (9)$$

$$I_s \cong \frac{S}{R_r}V_s \quad (10)$$

Thus, near synchronous speed, torque and the load component of current are essentially proportional to slip. The proportionality between torque and slip is indicated in Fig. 7 by broken line passing through the point (ω_e, 0). Since equation (8) shows that for constant applied terminal potential difference, torque is a function of slip only, then maximum and minimum values of torque and the slip S at which they occur are determined by setting $dT_e/ds = 0$ and solving for S. The solution is

$$S_{\max} = \pm\frac{R_r}{\sqrt{R_s^2 + \omega_e^2(L_{ls} + L_{lr})^2}}. \quad (11)$$

Substitution of the positive value of S from equation (11) in equation (8) gives the maximum torque,

$$T_{\max} = \frac{3}{2}\frac{p}{2}\frac{1}{\omega_e}\frac{V_s^2}{\sqrt{R_s^2 + \omega_e^2(L_{ls} + L_{lr})^2} + R_s}. \quad (12)$$

It is noted that, at large values of slip S, $\omega_e(L_{ls} + L_{lr}) >> R_s + R_r/S$, and equation (8) can be approximated by

$$T_e \cong 3\frac{p}{2}\frac{R_r}{S\omega_e}(\frac{V_s}{\omega_e(L_{ls} + L_{lr})})^2. \quad (13)$$

That is, the electro-magnetic torque is inversely proportional to slip, as shown by the curve in Fig. 7. Substitution of S=1 in (8) gives the locked-rotor or starting torque of the motor as

$$T_e = 3\frac{p}{2}\frac{1}{S\omega_e}\frac{R_r V_s^2}{(R_s + R_r)^2 + \omega_e^2(L_{ls} + L_{lr})^2}. \quad (14)$$

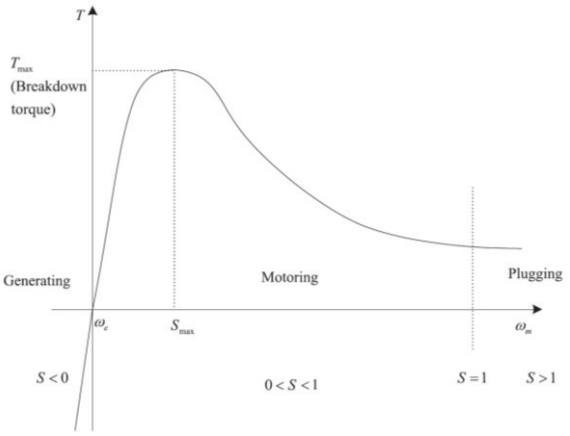

Fig. 7. Speed-Torque curve of an induction machine.

From equation (5), the real part which is expressed by current magnitude and displacement angle is written as

$$I_s\cos\phi = \mathrm{Re}[\mathbf{I_s}] = \frac{(R_s + R_r/S)V_s}{(R_s + R_r/S)^2 + \omega_e^2(L_{ls} + L_{lr})^2} \quad (15)$$

where ϕ is a displacement angle of stator current. From equation (15), a second order equation as for slip S expressed as

$$aS^2 + bS + c = 0 \tag{16}$$

where

$$\begin{aligned} a &= V_s R_s - I_s \cos\phi (R_s^2 + \omega_e^2 (L_{ls} + L_{lr})^2) \\ b &= V_s R_r - 2R_s R_r I_s \cos\phi \\ c &= -R_r^2 I_s \cos\phi. \end{aligned} \tag{17}$$

Thus the meaningful solution, slip S, is given by

$$S = \frac{-b + \sqrt{b^2 - 4ac}}{2a}. \tag{18}$$

This solution is expressed by real component of stator current and also using imaginary component of stator current is feasible solution. However if the magnitude of stator current is only used, a forth order equation as for slip S is made. Hence, estimating slip is more complicated and this method is nowhere near the simplified scheme.

The imaginary component of the stator current can be written as

$$I_s \sin\phi = \mathrm{Im}[\mathbf{I_s}] = -\frac{V_s}{\omega_e L_m} - \frac{\omega_e (L_{ls} + L_{lr}) V_s}{(R_s + R_r / S)^2 + \omega_e^2 (L_{ls} + L_{lr})^2}. \tag{19}$$

In the same way, a second order equation as for slip S is expressed as

$$a'S^2 + b'S + c' = 0 \tag{20}$$

where

$$\begin{aligned} a' &= \omega_e L_m I_s \sin\phi (R_s^2 + \omega_e^2 (L_{ls} + L_{lr})^2) + R_s^2 + \omega_e^2 (L_{ls} + L_{lr})(L_{ls} + L_{lr} + L_m) \\ b' &= 2R_s R_r (1 + \omega_e L_m I_s \sin\phi) \\ c' &= R_r^2 (\omega_e L_m I_s \sin\phi + 1). \end{aligned} \tag{21}$$

Thus the solution, slip S, is given by

$$S = \frac{-b' + \sqrt{b'^2 - 4a'c'}}{2a'}. \tag{22}$$

However using imaginary component of stator current need more calculation and also for fluid load application, which is vacuum pump, it is needed monitoring real power directly calculated by real component. Therefore using real part of stator current is better than imaginary part. Fig. 8 shows the slip S versus $I_s cos\phi$. The slip S is determined by both stator current amplitude and displacement angle. Through either stator current amplitude or displacement angle is changed, it has influence on estimating the slip S. It is better than using only stator current amplitude. By using mapping referred to Fig. 8, the slip S is easily estimated.

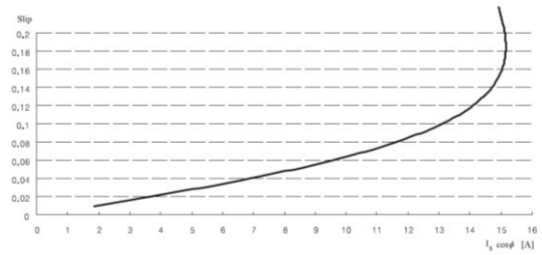

Fig. 8. Slip contour for an increasing the real component of stator current.

IV. Configuration of Controller

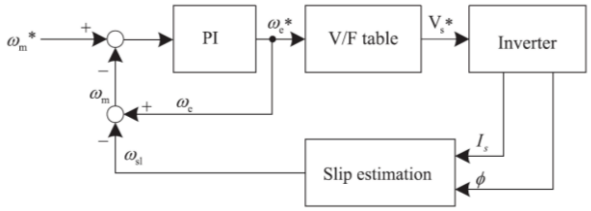

Fig. 9. Overall control block diagram.

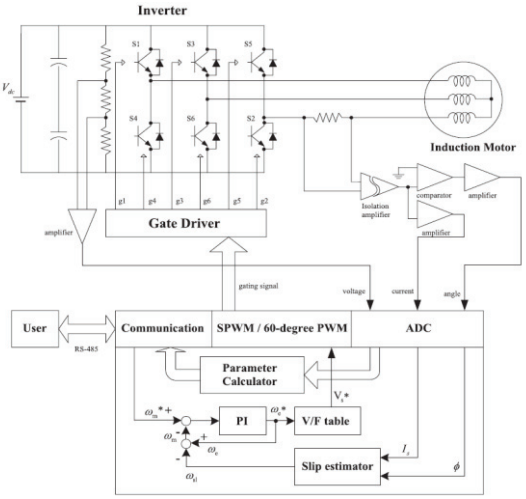

Fig. 10. Overall control structure.

The proportional-integral (PI) control scheme has been widely used for the speed control of motor drives. In this application, PI control scheme is used as the speed controller. The displacement angle and stator current amplitude are acquired and the slip S is estimated from these information. The mechanical angular frequency is calculated from slip. Fig. 9 shows overall block diagram for vacuum pump based on slip estimation. In the block diagram, parameters with superscript * denote command value. ω_m, ω_e and ω_{sl} denote mechanical, electrical and slip angular frequency, respectively. For slip estimation, Fig. 8 is applied and Speed controller is constructed with PI controller. V/F table is selected by electrical angular frequency. In the region of over-modulation, 60- degree PWM is adopted. Fig. 10 shows overall control structure for vacuum pump based on slip estimation where ADC is analogue to Digital converter. In the structure, isolation OP-amp is used for current sensing.

V. Experimental Results

Fig. 11 shows the block diagram of the experimental setup. The desktop-1 commands speed to the inverter by RS-485 serial communication and measures input parameters (current, power, torque, speed, temperature) to the motor. A power measuring device was installed at the input lines of the motor to measure the input power, current, voltage and power factor to the motor. The desktop-2 for measuring pressure was installed. The photos of the experimental setup are shown in Fig. 12.

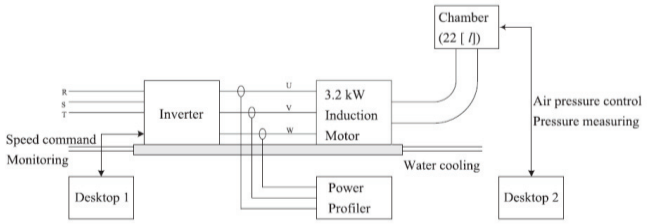

Fig. 11. Block diagram of the experimental setup.

TABLE I. Induction Motor Parameters

Description	Unit	Value
Rated power	HP	4.3 (3.2kW, 2pole)
Rated current	A_{rms}	12.1
Rated speed	rpm	5,640
R_s	Ω	0.517
R_r	Ω	0.652
L_m	mH	44.36
L_s	mH	47.07
L_r	mH	48.08

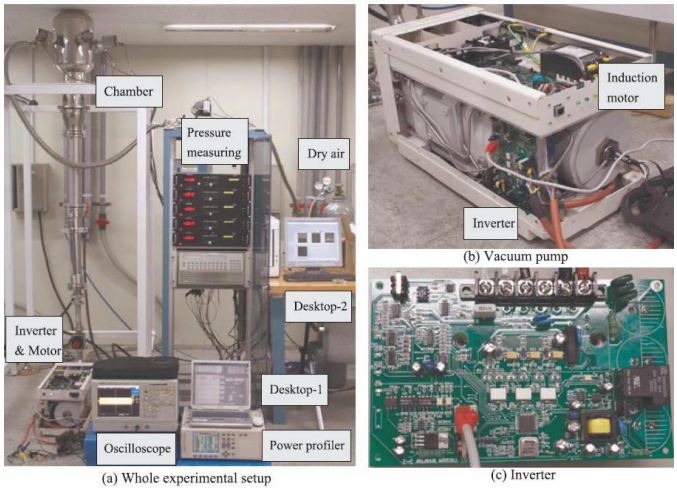

Fig. 12. Photos of the experimental setup.

The PWM frequency was 4.0 kHz and the dead-time was 2 μs. The whole algorithms for control were implemented using a PIC18F4431 integer microprocessor. After dry air was filled in a chamber (22 l) until air pressure is 1 atm (760 mmHg), a valve was opened in order to measure parameters. The time which is under 0.5 mmHg is tact time.

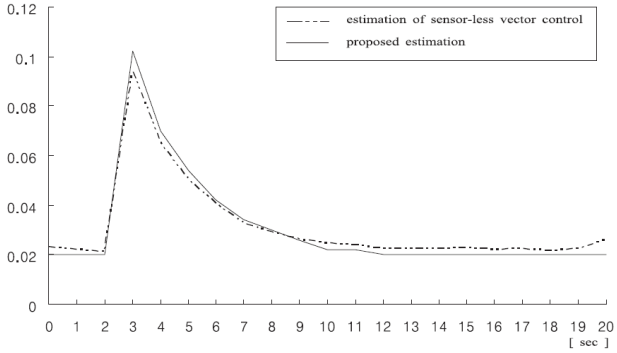

Fig. 13. Comparison between slip estimation of conventional sensor-less vector control and proposed slip estimation.

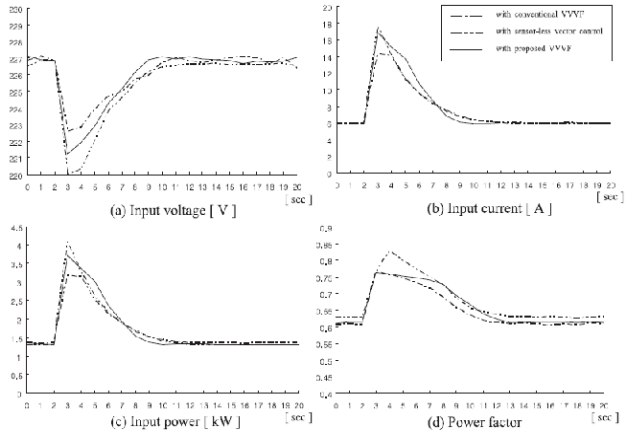

Fig. 14. Experimental results of voltage, current, power, and power factor when the pressure is 760 mmHg.

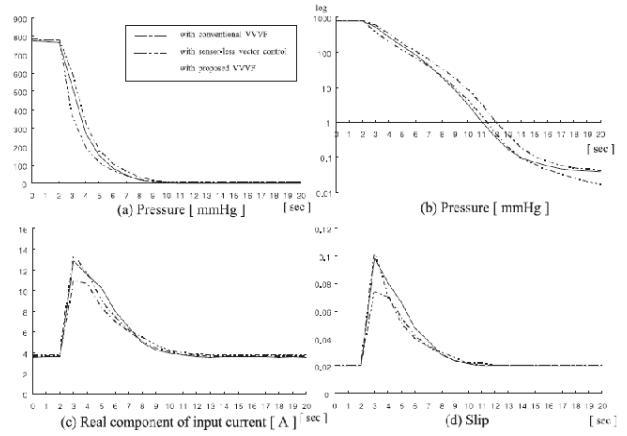

Fig. 15. Experimental results of pressure, pressure (log scale), real component of current, and slip when the pressure is 760 mmHg.

Fig. 13 shows slip estimated by conventional sensor-less vector control and slip by proposed estimation. By mapping applied the proposed scheme, the slip was estimated. Though it is not considered inductance variation and transient state, the results show that the proposed slip estimation are comparatively satisfactory as shown in Fig. 13.

To compare the performance, two kinds of inverter which are developed inverter and general-purpose inverter were used. We will call general-purpose inverter based on sensor-less vector control. Developed inverter was operated by two cases of control scheme which are general open-loop V/F control scheme and proposed slip estimation V/F control scheme. We will call general open-loop V/F control scheme as conventional V/F, and proposed slip estimation V/F control scheme as proposed V/F.

Fig. 14 and Fig. 15 show the experimental results of voltage, current, power, power factor, pressure, real component of current, and slip when the pressure control valve was opened at rated speed (6,000 rpm). All parameters were measured every one second. From Fig. 14 (a), voltage generated is almost same under steady state. And tact time of conventional V/F is 11 sec and tact time of vector controlled inverter and proposed V/F is almost same as 10 sec.

VI. Conclustion

The efficiency of motors for vacuum pump are lower than others because of large air-gap to keep vacuum state. For the operation of a vacuum pump which has small capacity, it is important to consider not only the performance but also the cost. In order to simplify the circuit, V/F scheme based on simplified slip estimation was proposed and 60-degree modulation was applied for high voltage utilization. An induction motor dynamics for vacuum pump was simplified at the steady state. In the simplified model, the slip was estimated by input current of the motor. According to the calculation and experimental results, the tact time based on this simplified slip estimation was fewer than conventional open-loop V/F scheme. Even though it has compared with general-purpose inverter based on sensor-less vector control, the tact time is better. A difference from previous work is that the proposed model did not consider the change of inductance. However the performance which keep down air pressure was good enough. The experimental results demonstrated the effectiveness of the proposed ideas.

Acknowledgment

This research was financially supported by the Ministry of Trade, Industry and Energy (MOTIE) and Korea Institute for Advancement of Technology (KIAT) through the Development for Design Convergence Micro-mobility Industry Ecosystem. (A007700014)

References

[1] G.R. Slemon, and A. Staughen, Electric Machines, Addison-Wesley, 1982.

[2] Gordon R.Slemon, Electric Machines and Drives, Addison-Wesley, 1992.

[3] Gary S. May, and Simon M. Sze, Fundamentals of Semiconductor Fabrication, Addison-Wesley, 2004.

[4] M. Beck and D. Naunin, “Slip frequency and sensorless control of induction motors,” Proc. of 4th Ann. Mtg. PPL Conf., pp.179-181, 1985.

[5] C. Schauder, ”Adaptive speed identification for vector control of induction motors without rotational transducers,” IEEE Trans. Ind. Applicat., vol.28, pp.1054-1061, Sep/Oct. 1992.

[6] A. Abbondanti and M.Brennen, ”Variable speed induction motor drives use electronic slip calculator based on motor voltages and currents,” IEEE Trans. Ind. Applicat., vol. IA-11, pp. 483-488, Sept. 1975.

[7] R. Joetten and G. Maeder, ”Control methods for good dynamic performance induction motor drives based on current and voltage as measured quantities,” lEEE Trans. Ind. Applicat., vol. IA-19, pp. 356-362, May 1983.

[8] Nicholas P.Rubin, Ronald G.Harley and Gregory Diana, ”Evaluation of various slip estimation techniques for an induction machine operating under field-oriented control conditions,” IEEE Trans. Ind. Applicat., vol.28, pp.1367-1375,Nov/Dec. 1992.

[9] Tajima, H. and Hori, Y., ”Speed sensorless field-orientation control of the induction machine,” IEEE Trans. Ind. Applicat., Vol.29, Issue 1, pp.175-180, Jan-Feb. 1993.

[10] Ned Mohan, Tore M.Undeland, William P.Robbins, Power Electronics, John Wiley and Sons, Inc. 1995.

[11] D.W.Novotny and T.A.Lipo, Vector Control and Dynamics of AC Drives, Oxford: Clarendon Press, 1996.

[12] Muhammad H.Rashid, Power Electronics, Pearson Education International, 2004.